

# End-To-End Procedure For IORT in Brain Metastases and Film Dosimetry

Sergio Lozares-Cordero, Reyes Ibáñez-Carreras<sup>1</sup>, Alberto García-Barrios<sup>2</sup>, Raquel Castro-Moreno, Andrea González-Rodríguez, Marta Sánchez-Casi, Arantxa Campos-Boned<sup>1</sup>, Almudena Gandía-Martínez, José Antonio Font-Gómez, Sara Jiménez-Puertas, David Villa-Gazulla, Javier Díez-Chamarro, Mónica Hernández-Hernández, Víctor González-Pérez<sup>3</sup>, Ana Isabel Cisneros-Gimeno<sup>2</sup>

Department of Physics and Radiation Protection, Miguel Servet University Hospital, Zaragoza, <sup>1</sup>Department of Radiation Oncology, Miguel Servet University Hospital, Zaragoza, <sup>2</sup>Department of Anatomy and Histology, School of Medicine, University of Zaragoza, <sup>3</sup>Department of Medical Physicist, IVO Foundation, Valencia, Spain

## Abstract

**Purpose:** The study is intended to perform an end-to-end test of the entire intraoperative process using cadaver heads. A simulation of tumor removal was performed, followed by irradiation of the bed and measurement of absorbed doses with radiochromic films. **Materials and Methods:** Low-energy X-ray intraoperative radiotherapy (IORT) was used for irradiation. A computed tomography study was performed at each site and the absorbed doses calculated by the treatment planning system, as well as absorbed doses with radiochromic films, were studied. **Results:** The absorbed doses in the organs at risk (OAR) were evaluated in each case, obtaining maximum doses within the tolerance limits. The absorbed doses in the target were verified and the deviations were <1%. **Conclusions:** These tests demonstrated that this comprehensive procedure is a reproducible quality assurance tool which allows continuous assessment of the dosimetric and geometric accuracy of clinical brain IORT treatments. Furthermore, the absorbed doses measured in both target and OAR are optimal for these treatments.

**Keywords:** End-to-end test, intraoperative radiotherapy, radiochromic film

Received on: 14-02-2023

Review completed on: 14-05-2023

Accepted on: 18-05-2023

Published on: 29-06-2023

## INTRODUCTION

In recent decades, improved systemic treatment options have led to prolonged survival of patients suffering from metastatic cancer of many tumor types (e.g., malignant melanoma, colorectal carcinoma, and lung cancer), including patients with brain metastases. Brain metastases are the most common intracranial tumor in adults, affecting up to 30% of adult cancer patients.<sup>[1]</sup> Treatment options include surgical resection with adjuvant radiotherapy (RT) and cancer-specific medical therapy.<sup>[2]</sup> Historically, the prognosis has been dismal, with a median survival of 1 month without treatment, 4–6 months with adjuvant RT, and 7–8 months with adjuvant RT, modern systemic therapy (chemotherapy and targeted therapy), and supportive care.<sup>[3]</sup> In view of this, other modalities of radiation delivery have been investigated for brain metastases.

In the early 1990s, the median survival of a carefully selected subset of patients treated with resection of a single-brain metastases followed by whole-brain RT (WBRT) was 9.2 months.<sup>[2]</sup> In another series of patients undergoing surgery

and focused RT for brain metastases, median survival even exceeded 24 months.<sup>[4]</sup> As most of these patients lived more than 1 year after brain metastases treatment, long-term local control, and treatment-related long-term neurotoxicity had gained increasing importance. Several trials have shown the detrimental effect of WBRT on neurocognitive functioning.<sup>[5,6]</sup> This led to a shift of paradigm in RT treatment after resection of brain metastases, away from WBRT and towards targeted irradiation of the resection cavity.<sup>[7,8]</sup>

Intraoperative RT (IORT) is the delivery of ionizing radiation to the tumor or tumor bed during surgery while the targeted tissue is exposed.<sup>[9]</sup> In contrast to other radiation modalities, such as WBRT, external beam RT (EBRT), and stereotactic radiosurgery (SRS), and IORT has the advantage of increased

**Address for correspondence:** Dr. Sergio Lozares-Cordero, Isabel La Católica 1-3, Zaragoza 50009, Spain.  
E-mail: slozares@salud.aragon.es

This is an open access journal, and articles are distributed under the terms of the Creative Commons Attribution-NonCommercial-ShareAlike 4.0 License, which allows others to remix, tweak, and build upon the work non-commercially, as long as appropriate credit is given and the new creations are licensed under the identical terms.

**For reprints contact:** WKHLRPMedknow\_reprints@wolterskluwer.com

**How to cite this article:** Lozares-Cordero S, Ibáñez-Carreras R, García-Barrios A, Castro-Moreno R, González-Rodríguez A, Sánchez-Casi M, *et al.* End-to-end procedure for IORT in brain metastases and film dosimetry. *J Med Phys* 2023;48:175-80.

### Access this article online

Quick Response Code:



Website:  
www.jmp.org.in

DOI:  
10.4103/jmp.jmp\_18\_23

precision and minimal radiation exposure to adjacent normal tissues,<sup>[10]</sup> thereby minimizing side effects.

IORT has emerged as a viable tool for the delivery of adjuvant treatment following tumor resection. The safety of IORT in the setting of glioblastoma has been established in conjunction with the addition of EBRT to the Stupp protocol and its efficacy is being evaluated in a Phase III clinical trial.<sup>[11]</sup> Unfortunately, the published data regarding the use of IORT for surgically-resected brain metastases are limited to single institutional studies.<sup>[12-14]</sup> Moreover, recent evidence suggests that the dose delivered locally to the resection cavity may have escalated beyond that safely achievable with traditional SRS techniques, although eliminating delay in time to initiation of radiation treatment following surgery and avoiding the complexity of target delineation in postoperative period.<sup>[13]</sup>

IORT with 50-kV X-rays is an alternative method to irradiate the resection cavity focally after neurosurgical resection of brain metastases.<sup>[14]</sup> Low-energy X-ray IORT uses a 30–50-kV isotropic X-ray source with either fixed diameter rigid spherical applicators (Intrabeam<sup>®</sup>, Carl Zeiss Meditec AG, Jena, Germany) or miniaturized X-ray source balloon applicators (Xoft<sup>®</sup>, San Jose, CA, USA). Allowing for excellent conformal apposition to the resection cavity walls, these devices exhibit a steep dose gradient with most of the dose delivered within 5–10 mm of the applicator surface. While the majority of clinical trial and outcome data using low-energy X-ray IORT have come from the management of breast cancer via the TARGIT studies,<sup>[15]</sup> recent clinical trials have involved glioblastoma and more widespread use in surgically resected intracranial metastatic disease.<sup>[11,16]</sup>

To date, known data regarding IORT in surgically treated brain metastases are limited to several single institutional studies indicating promising high rates of local tumor control and a low incidence of radiation necrosis.<sup>[16]</sup> These studies are mainly focused on treatment parameters, such as dosage, size of applicator, and time span of IORT procedures.<sup>[13,16,17]</sup>

While a range of quality assurance (QA) tests are performed on a regular basis to verify that clinical imaging systems, treatment planning systems (TPS), and treatment machines are operating as expected, these tests do not guarantee the accuracy of the overall treatment process and delivery. Modern RT treatments involve many interdependent processes, including computed tomography (CT) imaging, target delineation and contouring of organs at risk (OAR), treatment planning, data transfer between workstations and imaging and treatment units, patient positioning and immobilization, and finally dose delivery. Therefore, initiating routine end-to-end (E2E) QA would be useful to validate the entire treatment process.<sup>[18]</sup> Absorbed doses were measured in different areas of interest in the surgical bed, using a dosimetry system and radiochromic film. The aim of the project is to develop the necessary tools to ensure the quality of the overall process and to adapt the synergies of all the specialists involved, as well as to verify the absorbed doses both in the tumor bed and in the possible OAR.

## MATERIALS AND METHODS

The study consent was approved by the Aragonese Regional Health Service (Spain) and its ethics committee. Three heads of corps provided by the local school of medicine were used. Each of them simulates a lesion in different areas of the skull: frontal, occipital, and parietal locations [Figure 1].

Resection of a simulated tumor, 18–25 cm<sup>3</sup>, was performed just before treatment with IORT. Treatments were performed with Axxent low-energy X-ray equipment (Xoft<sup>®</sup>, San Jose, CA, USA).

This low-energy X-ray IORT system uses a miniaturized 50 kVp X-ray source with spherical “balloon” applicators. The tumor beds corresponding to 25, 20, and 18 cm<sup>3</sup> spherical applicators (the smallest available and most likely used in cases of brain metastases) were irradiated with a prescribed dose of  $20 \pm 0.1$  Gy on the applicator surface. A CT study was performed at each site and eyes, optical nerves, chiasm, brainstem, and lateral ventricle were contoured as OARs.

As part of the commissioning of the procedure, absorbed doses were measured at various locations in the surgical setting. Radiochromic film was used as a detector. In the present study, absorbed doses were measured using XR-RV3 radiochromic film, which is specific for energies from upward of 20 kVp and absorbed doses of up to 30 Gy.

Appropriate calibration of the films was ensured using a beam quality that is as close as possible to that used in the surgical procedure. Model XR-RV3 (batch 02141901) films were custom calibrated by cutting pieces of film measuring 5 cm × 5 cm. These were then appropriately marked and numbered to maintain their orientation in an Epson Expression 12000XL scanner. The protocol of Méndez *et al.*<sup>[19]</sup> was followed. The films used for the calibration were scanned before and after irradiation; postirradiation scanning was always performed 24 h later. The scanner was turned on 1 h before use, and five scans were made before scanning the films to warm up the light source, both before and after irradiation.

The films were scanned in red-green-blue (48-bit) reflection mode with a resolution of 75 dpi using Epson Scan software. The maximum range of optical density was applied, and all image corrections and filters were switched off.

All films were scanned in portrait orientation (scan direction is perpendicular to the coating direction), one by one, by placing the film in the center of the scanner. No correction was applied to address heterogeneity in the scanner response, since in no case was an area greater than 6 cm × 6 cm in the central part of the scanner. Uniformity was 0.3%, following the method used by Richter *et al.* with the EBT1 films and the Epson V750 scanner.<sup>[20]</sup> Each film was scanned consecutively 5 times and saved as a TIFF file. The scanned films were subsequently read and calibrated using the multichannel method with a multigaussian approach.<sup>[21]</sup>

The pieces of film (5 cm × 5 cm) were exposed to absorbed doses from 0 to 25 Gy, as the recommendation is to calibrate

up to 20% above the maximum to be measured (20 Gy in contact with the applicator).<sup>[22]</sup> Once the films were scanned, the files generated (both irradiated and nonirradiated films) were loaded into the Radiochromic.com v3.0 software application (Radiochromic SL, Benifaió, Spain).

A calibration curve using these images was calculated by selecting a region of interest of 1 cm × 1 cm, to which the dose value that had previously been calculated using a TM23342 PTW (PTW-Freiburg, Germany) ionization chamber was assigned. The software algorithm constructs the calibration curve that was used to measure the doses of the irradiated films used for the patients.<sup>[21]</sup> The calibrated batch of films (XR-RV3, batch 02141901) was cut in pieces (1 cm × 1 cm) and placed on/in the heads, which then underwent surgery and were treated *in situ* with the Axxent<sup>®</sup> device. A piece was placed on the surface of the “balloon” and at least 4 more were placed on the skin at different distances; the pieces were left in an opaque envelope for 24 h until scanning under the same conditions as the films used for calibration.

The files generated after five scans of each piece were loaded into the Radiochromic.com environment, where they were read using the previously generated calibration curves. After this process, the pieces of the film could be read in terms of dose.

The results were compared with the dose calculated by the Eclipse v 15.1 TPS (Varian Inc., Palo Alto, CA, USA). The calculation method used was as described in TG-43,<sup>[23]</sup> with specific parameters for the Axxent<sup>®</sup> system. The absorbed doses in the OAR were evaluated in each case, using Eclipse

v. 15.1 TPS (Varian Medical Systems, Palo Alto, CA, USA) [Figure 2].

## RESULTS

Absorbed doses were verified with radiochromic films at the target and different distances from the applicator, and each of three locations by measuring on the cadaver head itself [Table 1].

Deviations were <1% at the target and <6.5% on average (3.2%–6.5%) at different distances from the applicator. In addition, absorbed doses were estimated in the OARs calculated in the TPS after performing CT on the heads. The results are shown by location [Table 2].

## DISCUSSION

The methodology described in this paper outlines an E2E audit process that aims to independently verify the entire low-energy photon IORT treatment procedure at our center, from imaging to dose delivery. Using three cadaver heads and radiochromic films, this E2E dose analysis evaluated the dose calculation results of the TPS.

The results obtained with the radiochromic film fall within the range of those obtained in previous studies for the same type of film and radiation source.<sup>[24]</sup> The absorbed doses measured at the applicator surface for treatment volumes (18, 20, and 25 cm<sup>3</sup>) are equivalent to those calculated in the TPS. At distances of 1, 2, and 3 cm from the applicator, the results



**Figure 1:** Cadaver heads with radiochromic films for absorbed dose measurements

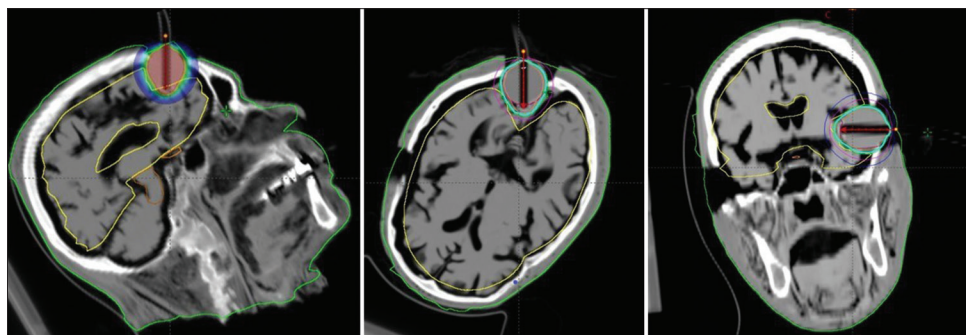


**Figure 2:** CT and isodose curves in frontal, occipital and parietal location. CT: Computed tomography

**Table 1: Clinical dose points**

Distance from target	Target (Gy)			1 cm (Gy)			2 cm (Gy)			3 cm (Gy)		
	TPS	RFD	Differ (%)	TPS	RFD	Differ (%)	TPS	RFD	Differ (%)	TPS	RFD	Differ (%)
TV: 18 cm <sup>3</sup>												
Frontal	20.2	20	1.0	8.1	7.8	3.7	3.7	3.5	5.4	2.2	2	9.1
Occipital	19.8	20	1.0	8	7.7	3.8	3.6	3.5	2.8	2.1	2.1	0.0
Parietal	19.9	20.1	1.0	8.2	7.9	3.7	3.7	3.4	8.1	2.1	1.9	9.5
Average	20.0	20.0	1.0	8.1	7.8	3.7	3.7	3.5	5.4	2.1	2.0	6.2
TV: 20 cm <sup>3</sup>												
Frontal	20	19.8	1.0	8.5	8	5.9	4	3.9	2.5	2.4	2.2	8.3
Occipital	20.1	19.9	1.0	8.2	7.9	3.7	3.9	3.7	5.1	2.5	2.4	4.0
Parietal	20	19.8	1.0	8.4	8.2	2.4	4	3.8	5.0	2.5	2.35	6.0
Average	20.0	19.8	1.0	8.4	8.0	4.0	4.0	3.8	4.2	2.5	2.3	6.1
TV: 25 cm <sup>3</sup>												
Frontal	20	20	0.0	8.5	8.2	3.5	4.1	4	2.4	2.6	2.3	11.5
Occipital	20.1	19.9	1.0	8.3	8	3.6	4.2	3.8	9.5	2.5	2.4	4.0
Parietal	20	20.1	0.5	8.2	8	2.4	4	3.8	5.0	2.5	2.4	4.0
Average	20.0	20.0	0.5	8.3	8.1	3.2	4.1	3.9	5.7	2.5	2.4	6.5

TPS versus dose measurements with radiochromic films for both treatment volumes (18 cm<sup>3</sup>, 20 cm<sup>3</sup>, and 25 cm<sup>3</sup>). TPS: Treatment planning system, RFD: Radiochromic film dosimetry, TV: Treatment volume

**Table 2: Absorbed doses in organs at risks calculated with treatment planning system for treatment volume of 18 cm<sup>3</sup>, 20 cm<sup>3</sup> and 25 cm<sup>3</sup>**

	Frontal		Occipital		Parietal	
	D <sub>max</sub> (Gy)	D <sub>mean</sub> (Gy)	D <sub>max</sub> (Gy)	D <sub>mean</sub> (Gy)	D <sub>max</sub> (Gy)	D <sub>mean</sub> (Gy)
TV: 18 cm <sup>3</sup>						
Right optical nerve	0.45	0.34	0.05	0.04	1.6	1.2
Left optical nerve	0.6	0.49	0.04	0.03	0.14	0.2
Right eye	0.48	0.25	0.02	0.01	1.32	0.6
Left eye	0.69	0.35	0.02	0.01	0.18	0.1
Chiasm	0.5	0.39	0.17	0.13	1.69	0.99
Brainstem	0.26	0.12	0.6	0.3	2.44	0.71
Lateral ventricle	2.5	0.59	1.2	0.2	1.84	0.68
TV: 20 cm <sup>3</sup>						
Right optical nerve	0.46	0.35	0.05	0.04	1.63	1.22
Left optical nerve	0.61	0.50	0.04	0.03	0.14	0.20
Right eye	0.49	0.26	0.02	0.01	1.35	0.61
Left eye	0.70	0.36	0.02	0.01	0.18	0.10
Chiasm	0.51	0.40	0.17	0.13	1.72	1.01
Brainstem	0.27	0.12	0.61	0.31	2.49	0.72
Lateral ventricle	2.55	0.60	1.22	0.20	1.88	0.69
TV: 25 cm <sup>3</sup>						
Right optical nerve	0.48	0.36	0.05	0.04	1.70	1.27
Left optical nerve	0.64	0.52	0.04	0.03	0.15	0.21
Right eye	0.51	0.27	0.02	0.01	1.40	0.64
Left eye	0.73	0.37	0.02	0.01	0.19	0.11
Chiasm	0.53	0.41	0.18	0.14	1.79	1.05
Brainstem	0.28	0.13	0.64	0.32	2.59	0.75
Lateral ventricle	2.65	0.63	1.27	0.21	1.95	0.72

D<sub>max</sub>: Maximum absorbed dose, D<sub>mean</sub>: Mean absorbed dose, TV: Treatment volume

remain similar, although the decrease of the reading and the higher uncertainty of the calculation method proposed by TG 43,<sup>[25]</sup> as we move away from the source, make the differences range from 4% to 6.5% on average for all treatment volumes at all locations, as in other published studies.<sup>[26]</sup> Differences

appear at distances of 2–3 cm for the same reason, although the absorbed doses measured at these points, 3 cm from the source, are 2.1 Gy<sup>-2</sup>, 6 Gy, which represent only 10%–12.5% of the prescribed dose. At 1 cm from the radiation source, where absorbed doses are higher (7.8–8.5 Gy), the differences

between measured and calculated values are below 4% on average (2.4%–5.9%), which enhances treatment safety, as these are the areas closest to the radiation source. The absorbed doses measured in the target are consistent with those calculated in the TPS, with differences of 0.5%–1% in all cases studied.

The absorbed doses calculated in the OARs by the TPS are within tolerances for these cases. The selected locations are close to the surface, as these are the cases we aim to treat in our hospital. Maximum doses of 2.5 Gy were observed in the brainstem and lateral ventricle in the frontal and lateral cases for a treatment volume of 20 cm<sup>3</sup>, and 2.6 Gy for 25 cm<sup>3</sup> in the same locations. As expected, due to the smaller treatment volume, the results for 18 cm<sup>3</sup> are somewhat lower for all OARs.

Although the process has been carried out with real heads, it is not certain that they will be available in the future and that these tests can be repeated periodically, therefore, substitute anthropomorphic phantoms are being sought for future tests.

The study has limitations due to not taking into account the possible movement of the applicator during treatment delivery, or possible patient movements, which are typical uncertainties in an operating room. This could lead to a discrepancy in the absorbed doses in the target and OARs. Adequate surgical field configuration, along with appropriate selection of the volume to be irradiated, would minimize these issues in clinical practice.

The motivation behind developing in-house E2E testing is that these techniques could provide critical QA that addresses an inherent feature of IORT. IORT techniques incorporate multiple processes, each demanding a complex interchange during which a patient's treatment may be modified at various points based on decisions by clinical staff who interprets information acquired during the treatment course. While physics QA would have been performed to validate the hardware used or systems in place at individual steps in the process (e.g., through machine QA), such conventional QA does not, by its nature, validate the overall treatment process.

Establishing regular in-house E2E QA within treatment clinics would facilitate regular validation of the processes involved in modern radiation therapy.

## CONCLUSIONS

A unique advantage to the E2E testing presented here is the ability to mimic the specific IORT process, as it would be applied to a patient, i.e., through the complete chain of required data transfer, analysis, and decision-making (steps that are often judgment-based and not tested in conventional physics QA procedures).

This study served as a commissioner for the entire brain IORT process, ensuring the quality of all stages of the process, from surgery to measurement of absorbed doses in target and OARs.

## Financial support and sponsorship

Nil.

## Conflicts of interest

There are no conflicts of interest.

## REFERENCES

- Nayak L, Lee EQ, Wen PY. Epidemiology of brain metastases. *Curr Oncol Rep* 2012;14:48-54.
- Patchell RA, Tibbs PA, Regine WF, Dempsey RJ, Mohiuddin M, Kryscio RJ, *et al.* Postoperative radiotherapy in the treatment of single metastases to the brain: A randomized trial. *JAMA* 1998;280:1485-9.
- Moravan MJ, Fecci PE, Anders CK, Clarke JM, Salama AK, Adamson JD, *et al.* Current multidisciplinary management of brain metastases. *Cancer* 2020;126:1390-406.
- Doré M, Martin S, Delpon G, Clément K, Campion L, Thillays F. Stereotactic radiotherapy following surgery for brain metastasis: Predictive factors for local control and radionecrosis. *Cancer Radiother* 2017;21:4-9.
- Brown PD, Ballman KV, Cerhan JH, Anderson SK, Carrero XW, Whitton AC, *et al.* Postoperative stereotactic radiosurgery compared with whole brain radiotherapy for resected metastatic brain disease (NCCTG N107C/CEC-3): A multicentre, randomised, controlled, phase 3 trial. *Lancet Oncol* 2017;18:1049-60.
- Scoccianti S, Ricardi U. Treatment of brain metastases: Review of phase III randomized controlled trials. *Radiother Oncol* 2012;102:168-79.
- Soffietti R, Abacioglu U, Baumert B, Combs SE, Kinhult S, Kros JM, *et al.* Diagnosis and treatment of brain metastases from solid tumors: Guidelines from the European association of neuro-oncology (EANO). *Neuro Oncol* 2017;19:162-74.
- Scharl S, Kirstein A, Kessel KA, Duma MN, Oechsner M, Straube C, *et al.* Cavity volume changes after surgery of a brain metastasis-consequences for stereotactic radiation therapy. *Strahlenther Onkol* 2019;195:207-17.
- Paunesku T, Woloschak GE. Future directions of intraoperative radiation therapy: A brief review. *Front Oncol* 2017;7:300.
- Calvo FA. Intraoperative irradiation: Precision medicine for quality cancer control promotion. *Radiat Oncol* 2017;12:36.
- Giordano FA, Brehmer S, Mürle B, Welzel G, Sperk E, Keller A, *et al.* Intraoperative radiotherapy in newly diagnosed glioblastoma (INTRAGO): An open-label, dose-escalation phase I/II trial. *Neurosurgery* 2019;84:41-9.
- Hsieh J, Elson P, Otvos B, Rose J, Loftus C, Rahmathulla G, *et al.* Tumor progression in patients receiving adjuvant whole-brain radiotherapy versus localized radiotherapy after surgical resection of brain metastases. *Neurosurgery* 2015;76:411-20.
- Vargo JA, Sparks KM, Singh R, Jacobson GM, Hack JD, Cifarelli CP. Feasibility of dose escalation using intraoperative radiotherapy following resection of large brain metastases compared to post-operative stereotactic radiosurgery. *J Neurooncol* 2018;140:413-20.
- Weil RJ, Mavinkurve GG, Chao ST, Vogelbaum MA, Suh JH, Kolar M, *et al.* Intraoperative radiotherapy to treat newly diagnosed solitary brain metastasis: Initial experience and long-term outcomes. *J Neurosurg* 2015;122:825-32.
- Vaidya JS, Baum M, Tobias JS, Wenz F, Massarut S, Keshtgar M, *et al.* Long-term results of targeted intraoperative radiotherapy (Targit) boost during breast-conserving surgery. *Int J Radiat Oncol Biol Phys* 2011;81:1091-7.
- Cifarelli CP, Brehmer S, Vargo JA, Hack JD, Kahl KH, Sarria-Vargas G, *et al.* Intraoperative radiotherapy (IORT) for surgically resected brain metastases: Outcome analysis of an international cooperative study. *J Neurooncol* 2019;145:391-7.
- Kahl KH, Balagiannis N, Höck M, Schill S, Roushan Z, Shiban E, *et al.* Intraoperative radiotherapy with low-energy x-rays after neurosurgical resection of brain metastases-an Augsburg university medical center experience. *Strahlenther Onkol* 2021;197:1124-30.
- Schreiner LJ. End to end QA in image guided and adaptive radiation therapy. *J Phys Conf Ser* 2019;1305:12062.
- Méndez I, Peterlin P, Hudej R, Strojnik A, Casar B. On multichannel film dosimetry with channel-independent perturbations. *Med Phys* 2014;41:011705.

20. Richter C, Pawelke J, Karsch L, Woithe J. Energy dependence of EBT-1 radiochromic film response for photon (10kVp-15MVp) and electron beams (6-18MeV) readout by a flatbed scanner. *Med Phys* 2009;36:5506-14.
21. Méndez I, Polšak A, Hudej R, Casar B. The Multigaussian method: A new approach to mitigating spatial heterogeneities with multichannel radiochromic film dosimetry. *Phys Med Biol* 2018;63:175013.
22. Lewis D, Micke A, Yu X, Chan MF. An efficient protocol for radiochromic film dosimetry combining calibration and measurement in a single scan. *Med Phys* 2012;39:6339-50.
23. Rivard MJ, Coursey BM, DeWerd LA, Hanson WF, Huq MS, Ibbott GS, *et al.* Update of AAPM task group no. 43 report: A revised AAPM protocol for brachytherapy dose calculations. *Med Phys* 2004;31:633-74.
24. Lozares S, Font JA, Gandía A, Campos A, Flamarique S, Ibáñez R, *et al.* *In vivo* dosimetry in low-voltage IORT breast treatments with XR-RV3 radiochromic film. *Phys Med* 2021;81:173-81.
25. Zehtabian M, Faghihi R, Si S. A Review on Main Defects of TG-43, Brachytherapy. *InTech*, 2012. doi: 10.5772/34360.
26. McCabe BP, Speidel MA, Pike TL, Van Lysel MS. Calibration of GafChromic XR-RV3 radiochromic film for skin dose measurement using standardized x-ray spectra and a commercial flatbed scanner. *Med Phys* 2011;38:1919-30.